

# Radio Science®

## RESEARCH ARTICLE

10.1029/2022RS007530

### Special Section:

Microwave and Millimeter Wave  
Propagation: Modeling and  
Applications

### Key Points:

- Results from a long-term D-band propagation experiment carried out in two sites (carrier frequency 156 GHz) are processed and presented
- Rain attenuation prediction models are tested against the experimental data, both on an event basis and on a statistical basis

### Correspondence to:

A. M. Musthafa,  
ashifa0430@gmail.com

### Citation:

Musthafa, A. M., Luini, L., Riva, C., Livieratos, S. N., & Roveda, G. (2023). A long-term experimental investigation on the impact of rainfall on short 6G D-band links. *Radio Science*, 58, e2022RS007530. <https://doi.org/10.1029/2022RS007530>

Received 21 JUN 2022

Accepted 5 APR 2023

### Author Contributions:

**Conceptualization:** Lorenzo Luini  
**Data curation:** Ashifa M. Musthafa, Spiros N. Livieratos  
**Formal analysis:** Carlo Riva  
**Funding acquisition:** Lorenzo Luini, Carlo Riva, Spiros N. Livieratos  
**Investigation:** Ashifa M. Musthafa, Spiros N. Livieratos  
**Methodology:** Lorenzo Luini  
**Project Administration:** Lorenzo Luini  
**Resources:** Giuseppe Roveda  
**Software:** Ashifa M. Musthafa  
**Supervision:** Giuseppe Roveda  
**Validation:** Ashifa M. Musthafa, Spiros N. Livieratos  
**Writing – original draft:** Ashifa M. Musthafa  
**Writing – review & editing:** Lorenzo Luini, Carlo Riva, Spiros N. Livieratos, Giuseppe Roveda

## A Long-Term Experimental Investigation on the Impact of Rainfall on Short 6G D-Band Links

Ashifa M. Musthafa<sup>1</sup> , Lorenzo Luini<sup>1</sup> , Carlo Riva<sup>1</sup>, Spiros N. Livieratos<sup>2</sup>, and Giuseppe Roveda<sup>3</sup>

<sup>1</sup>Dipartimento di Elettronica, Informazione e Bioingegneria, Politecnico di Milano, Milan, Italy, <sup>2</sup>Department of Electrical and Electronic Engineering, School of Pedagogical and Technological Education Heraklion, Heraklion, Greece, <sup>3</sup>Huawei Technologies S.r.l, Segrate, Italy

**Abstract** Results from a long-term propagation campaign are presented, whose main goal is to investigate the impact of rainfall on short terrestrial links operating at frequencies in the D-band, to be possibly exploited for backhaul links in future 6G mobile networks. To this aim, data are collected at two sites with different climatic conditions (Milan, Italy; Athens, Greece) for 24 and 20 months, respectively, using two links (path length of 325 and 100 m, respectively), operating at 156 GHz carrier frequency. At the same sites, disdrometers are also installed to concurrently collect information on precipitation, not only in terms of rain rate but also of its microphysical properties. The received power data are carefully pre-processed to exclude outliers and further elaborated to derive the rain attenuation. The data are afterward used to evaluate the accuracy of different prediction models, both on an event basis and on a statistical basis. Results indicate that the information delivered by the Drop Size Distribution allows a more accurate estimation of the rain attenuation and that the model currently adopted by the ITU-R to predict rain attenuation statistics on terrestrial links (recommendation ITU-R P.530-18) yields a significant overestimation for such short links, due to the unrealistic value of its path reduction factor. On the contrary, the statistical prediction model proposed by Lin turns out to offer a very satisfactory prediction accuracy.

## 1. Introduction

The D band, extending from 130 to 175 GHz, is currently being considered a potential candidate to enable 6G communications (Zhang et al., 2019) (Saad et al., 2020). Thanks to its large bandwidth, it is expected to support the continuous increase in traffic and provide ultra-fast data rates (up to 100 Gb/s), in compliance with the upcoming network requirements (Kim & Zajic, 2015). On the other hand, the detrimental effects that the atmosphere induces on electromagnetic (EM) waves quickly increase as we shift to the higher portion of the spectrum. The influence of gas (water vapor and oxygen), suspended water droplets (fog), and hydrometeors (e.g., hail, snow, and rain) play a significant role in causing impairments to EM propagation at higher bands (Paraboni et al., 2002). Among these, rainfall causes the strongest deterioration to the signal as the raindrop dimensions are comparable in size to the wavelength, specifically inducing scattering and absorption of the incident EM wave. Hence, it is necessary to investigate the effects of rain on the propagating EM waves, even more so because, at higher frequencies, the estimation of the impact of precipitation becomes complex due to the dependence of the specific attenuation on the shape and dimension of raindrops. This goal can be achieved by means of theoretical studies, such as those presented in Pérez-Pena et al. (2021) and Pimienta-del-Valle et al. (2022), where the information on the microphysical properties of rainfall is used to accurately estimate the induced attenuation in the 80–200 GHz band. On the other hand, it is also vital to conduct propagation experiments, which represent the first key step for the development of propagation models aimed at predicting the statistics of the rain attenuation affecting terrestrial links. Some previous experiments focused on characterizing the indoor channels at D band (Chen & Cao, 2013) (Kim et al., 2015), while (Ishii et al., 2016) investigated the impact of rain attenuation on links at D band, but only on a short-term basis (2 months) and considering quite a limited precipitation intensity (11 mm/hr maximum). To the best of our knowledge, no long term outdoor propagation experiment at D band has been conducted yet.

Originating from the collaboration between Politecnico di Milano and the Huawei European Microwave Centre in Milan, this research activity aims at filling this gap by investigating the effect of the atmosphere on two D-band terrestrial links. The experimental setup in Milan, Italy, consists of a 325 m D-band link operating with a carrier frequency equal to 156 GHz used to investigate the effect of rain attenuation, starting from the received power.

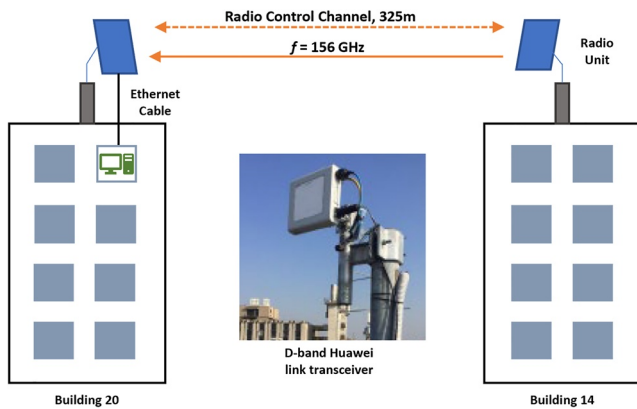


**Figure 1.** Architecture of the Huawei D-Band link in Milan.

This goal is aided by the ancillary data collected by meteorological instruments (weather station and disdrometer) close to the experimental site. The rain attenuation data are then used to assess the accuracy of some rain attenuation time series models, as well as the performance of statistical prediction methods, including the one adopted by the International Telecommunication Union—Radiocommunication Sector (ITU-R) in Recommendation ITU-R P.530-18 (ITU-R P.530-18, 2021) and the Lin model (Lin, 1977). Additional data, included in this contribution, have been obtained from another Huawei experimental D-band link, set up in Athens, Greece. This link, operating with the same carrier frequency at 156 GHz, has a path length approximately 100 m and is installed alongside a disdrometer to measure the local rain rate. The remainder of this paper is organized as follows. Section 2 describes the setup of the two experimental links; Section 3 presents the data processing steps taken to derive rain attenuation from the received power; Section 4 and Section 5 deal with prediction models, on an event basis and on a statistical basis. Finally, Section 6 draws some conclusions and outlines the future work.

## 2. Experimental Setup

### 2.1. Experimental Setup in Milan

The experimental setup in Milan consists of a 325-m D-band link operating with a carrier frequency of 156 GHz and a channel bandwidth of 250 MHz. Specifically, as depicted in Figure 1, the link consists of a transmitter, installed on the rooftop of Building 14, and of a receiver, installed on the rooftop of Building 20 (both buildings are located in the Politecnico di Milano main campus). The transmit power is sampled and gathered at the receiver side through the radio control channel; this information is stored on a PC connected via Ethernet to the receiver outdoor unit, which also collects the received power (5 samples/s). All the data are time-stamped with UTC time and stored in CSV files in the monitoring PC. The link has been operational since 2016, but in this work, we make use of the data recorded from 1 February 2018 to 31 January 2020: in fact, since the beginning of February, the data quality has significantly improved thanks to the installation of a cover, both on the transmitter side and on the receiver side, which prevents rain from falling directly on the antenna, which, in turn, eliminates the wet antenna effect problem. Table 1 provides additional detail on the D-band link transceivers (Luini et al., 2018).

As is well known, the attenuation due to rain depends not only on the rain rate but also on the shape and size of raindrops (Lam et al., 2012). The latter information is typically provided by the so-called Drop Size Distribution (DSD), which is measured by disdrometers. In this research activity, the Thies CLIMA laser precipitation monitor (LPM), installed on the rooftop of Building 20 at 10 m from the link receiver, is used to collect DSD data, which, in turn, are useful to support the prediction of specific rain attenuation (as explained in more detail in Section 4.2 below). The LPM operates by means of an infrared beam (785 nm) covering an area of 4,560 mm<sup>2</sup> (Thies Clima Laser Precipitation Monitor, 2011): the photodiode at the receiver side monitors the signal power fluctuations as precipitating particles cross the beam. Using this information, the particle diameter is derived. The LPM operates with a 1-min integration time.

Besides rain, also gases, mainly water vapor and oxygen in the 1–1,000 GHz range, induce attenuation on EM waves, which can be accurately estimated using mass absorption models, such as the one included in Annex 1 of recommendation ITU-R P.676 (ITU-R P.676-12, 2019), ITU-R Recommendation P.676-12 (2019), fed by some meteorological information. To this aim, the experimental campaign includes the collection of pressure ( $P$ ), temperature ( $T$ ), and relative humidity (RH) data, which are retrieved from the weather station located in Milano Linate airport (30-min sampling time), at just 5 km from the experimental site. Given the low spatial (order of kilometers) and temporal (order or tens of minutes) variability of  $P$ ,  $T$ , and RH, such data are considered representative of the experimental site.

**Table 1**  
System Parameters of the D-Band Link in Milan

Channel bandwidth	250 MHz
Transmitter power	+5 dBm
Receiver sensitivity	−67 dBm with QPSK
Antenna gain (both TX and RX)	34 dBi
Wave polarization	Linear vertical
Carrier frequencies	156 GHz
Atmospheric fade margin	15 dB

**Table 2**  
System Parameters of the D-Band Link in Athens

Channel bandwidth	250 MHz
Transmitter power	0 dBm
Receiver sensitivity	−67 dBm with QPSK
Antenna gain (both TX and RX)	33 dBi
Wave polarization	Linear vertical
Carrier frequencies	156 GHz
Atmospheric fade margin	17 dB

## 2.2. Experimental Setup in Athens

The experimental setup in Athens consists of a 100-m D-band link of Frequency Division Duplex technology operating with a carrier frequency of 156 GHz and a channel bandwidth of 250 MHz. Data were collected in a similar way as in Milan, though the period is different: in Athens, the link data were recorded from 1 October 2019 to 31 May 2021. The main difference lies in the unavailability of DSD data. Rain rate measurements are recorded with a 1-min integration time. Table 2 provides additional details on the D-band link transceivers installed in Athens. Finally, the meteorological data are collected from the nearest weather station.

## 3. Data Processing

### 3.1. Pre-Processing Steps

Figure 2 summarizes the D-band data pre-processing flow. The timestamps of the received power ( $P_{RX}$ ) data are first converted from local time to UTC time for synchronization of all the instruments. Afterward, the  $P_{RX}$  data are carefully visually inspected to identify and remove possible sudden drops in the received power (outliers), examples of which are also shown in Figure 3. Such outliers, which correspond to 0.1% of the total database samples, are likely due to quick sudden loss of locks in the receiver. Following this step, the  $P_{RX}$  data, are averaged over 1 min to match the integration time of the disdrometer rain rate data: besides providing the same time basis for the different data sets, as shown in Figure 3, this step also allows significantly reducing the fast signal oscillations due to scintillations induced by turbulence.

### 3.2. Rain Attenuation Extraction

The isolation of rain attenuation from the received power is not a trivial task, as the latter is typically affected by a number of factors: in fact, besides atmospheric constituents, the oscillation of the  $P_{RX}$  also typically depends on system parameters, such as change in the antenna pointing due to strong winds, variation in the transmitted power, modification in the receiver chain gain due to temperature oscillations, etc. Thus, though the total atmospheric attenuation  $A_T$  can in principle be calculated by inverting the link budget equation, in practice, this is not possible due to all the system-induced effects mentioned above. A possible more accurate way of extracting rain attenuation from the  $P_{RX}$  is to consider that, in rain-free conditions,  $A_T$  depends only on the attenuation induced by gases  $A_G$ : if an accurate estimation of the latter is available, the received power can be elaborated such that  $A_T$  coincides with  $A_G$  when the link is not affected by rain. Afterward, rain attenuation can be extracted from  $A_T$  by removing the contribution due to gases. The overall processing procedure is explained in more detail in the remainder of this Section by making reference to a rain event.

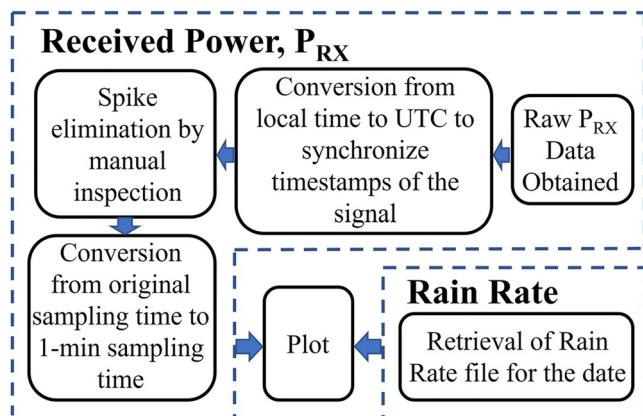


**Figure 2.** D-band data pre-processing flow.

Starting from the information of  $P$ ,  $T$ , and  $RH$ , the attenuation due to gases  $A_G$  is calculated using the model included in Annex 1 of Recommendation ITU-R P.676-12 (ITU-R P.676-12, 2019): specifically, the specific attenuation  $\gamma_G$  is calculated from  $P$ ,  $T$ , and  $RH$ , and, considering the low spatial variability of oxygen and water vapor along with the link, the path attenuation due to gases is simply calculated as  $A_G = \gamma_G L$ , where  $L$  is the link length. As an example, Figure 4 shows the gaseous attenuation at 156 GHz on 18 December 2019. As expected from (ITU-R P.676-12, 2019), the attenuation due to water vapor  $A_{wv}$  largely exceeds the one due to oxygen  $A_{ox}$ .

Figure 5 shows, for the same day as in Figure 4, the trend of the rain rate: as indicated by the red line, an event is simply identified when the rain rate  $R$  is higher than 0.05 mm/hr (lower values are assumed to be not reliable enough). For the correct extraction of rain attenuation, in the presence of rain events, the  $P_{RX}$  samples (the last sample before the rain event and the first sample after the rain event, as indicated in Figure 5) are interpolated with a 1-min interval step to obtain  $P'_{RX}$ : indeed, this step is important to identify the rain

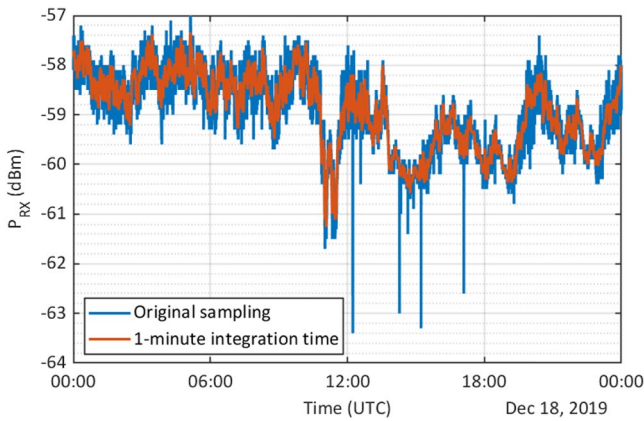


**Figure 3.** D-band signals ( $P_{RX}$ ) received on the 18 December 2019, in Milan: original sampling time and 1-min average.

contribution to the received power drop. Afterward,  $P'_{RX}$  is low pass filtered (0.025 Hz cut-off frequency) to remove the fast oscillations of the signal, thus obtaining  $P''_{RX}$  (yellow line in Figure 6). The following step consists in changing the sign of  $P_{RX}$  and forcing the agreement between  $P''_{RX}$  and  $A_G$ : the resulting total attenuation  $A_T$  is depicted in Figure 7, which points out how this procedure allows strongly mitigating the system-induced effects on  $A_T$ . The final step to derive rain attenuation  $A_R$  is to subtract  $A_G$  from  $A_T$  and to set to zero any residual value of  $A_R$  outside the rain event. The results, depicted in Figure 8, show that even quite a limited rain intensity, that is, between 2 and 3 mm/hr, can actually induce more than 2 dB of attenuation at the D band.

#### 4. Rain Attenuation Prediction: Time Series Analysis

This section presents different methods that can be used to predict the time series of the rain attenuation starting from information on precipitation; specifically: the approach based on the Recommendation ITU-R P.838-3

(ITU-R P. 838-3, 2005), ITU-R Recommendation P.838-3 (2005), which requires only the rain rate as input; the methodology taking full advantage of the DSD information. The two models are compared to the data on an event basis.

##### 4.1. Approach Based on Recommendation ITU-R P.838-3

A simple way of predicting the time series of the rain attenuation  $A_R$  is to use the simple power-law conversion between the rain rate  $R$  (mm/h) and the specific attenuation  $\gamma_R$  (dB/km) proposed by Recommendation ITU-R P.838-3, namely:

$$A_R^{ITU-R} = \gamma_R^{ITU-R} L = k R^\alpha L \quad (1)$$

Making reference to the D-band link in Milan, in Equation 1,  $L = 0.325$  km is the path length,  $R$  is the rain rate measured by the disdrometer (mm/hr), while  $k = 1.6014$  and  $\alpha = 0.6445$  are the conversion coefficients extracted from Recommendation ITU-R P.838-3, which depend on the wave frequency and polarization, as well as on the link elevation ( $0^\circ$  in this case). It is worth mentioning that this approach assumes that the rain rate, measured at the receiver side, is constant along the whole path: this hypothesis is definitely acceptable for stratiform events (roughly, when the peak rain rate does not exceed 10 mm/hr), while it might be more questionable for convective events; in this case, the introduction of a path reduction factor represents a simple yet effective way of taking into account the spatial inhomogeneity of the rain rate along the path (more details are discussed in Section 5).

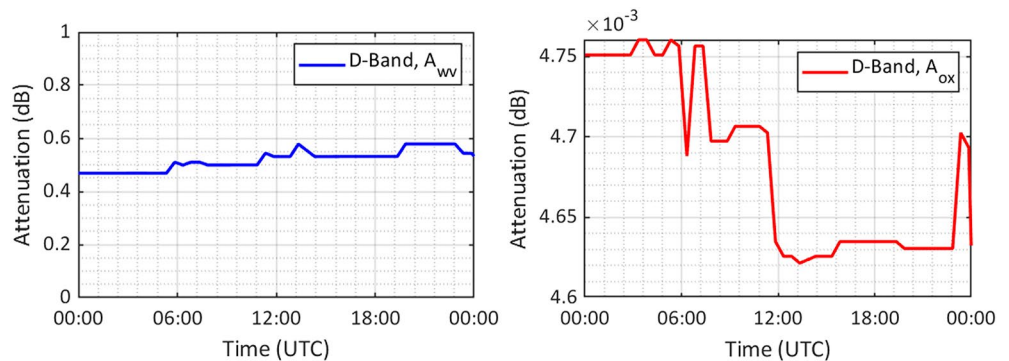


**Figure 4.**  $A_G$  estimated along the D-band link from local measurements in Milano Linate using Annex 1 of Recommendations ITU-R P.676-12.



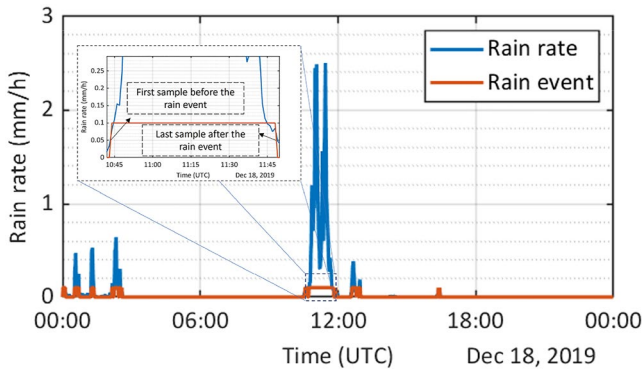


**Figure 5.** Measured rain rate on the 18 December 2019, in Milan.

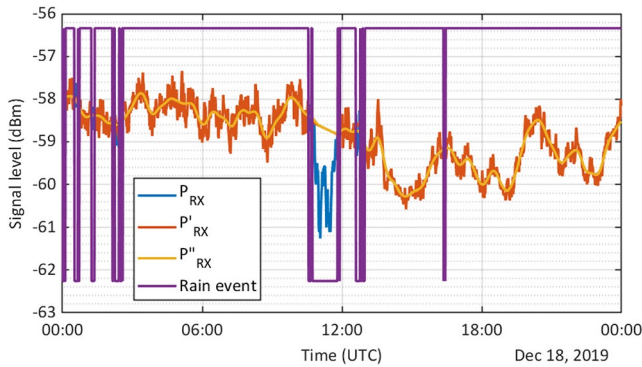


**Figure 6.** Processed  $P_{RX}$ ,  $P'_{RX}$ , and  $P''_{RX}$  on the 18 December 2019, in Milan.

10:30 UTC, both predictions are in good agreement with the link data. However, as the rain rate increases, the discrepancy between the two models clearly emerges: around 11:00 UTC, the DSD offers an accurate prediction (the error is roughly 0.2 dB for the rain attenuation peaks), while the ITU-R P.838-3 based method underestimates the measurements by more than 1.4 dB. This is just an example of how the attenuation due to rain is sensitive to the DSD at D band. Similar results are reported in Figure 10 for a sample rain event occurred in Athens (16 February, 2021): the rain attenuation estimated using the ITU-R P.838-3 based method tends to underestimate the measured data; as mentioned above, the more accurate model reported in Figure 9 is not applicable in this case, as no DSD data are available for Athens.

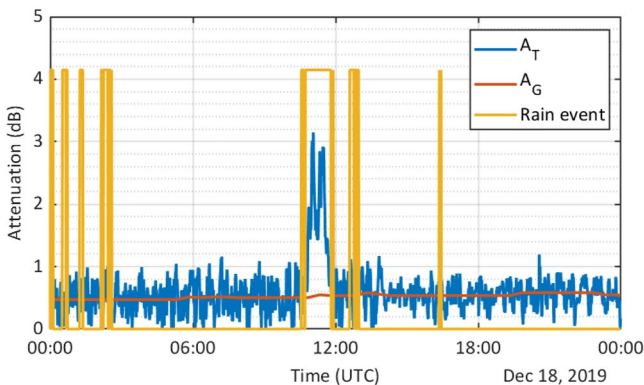


**Figure 7.** Time series of the total attenuation  $A_T$  and of the reference gaseous attenuation  $A_G$  (18 December 2019, in Milan).

## 4.2. Approach Based on the DSD

Each raindrop scatters and absorbs a given amount of EM energy depending on the water temperature (on which the electric permittivity depends), the wave polarization, and, mainly, the ratio between the wavelength and the drop diameter. As a consequence, using the information on the DSD is expected to be the most accurate approach to estimate the impact of rain: in fact, the same rain rate value can be obtained with quite different DSDs, resulting in different rain attenuation values. Using this methodology, the rain attenuation along the path can be calculated as (Lam et al., 2012):

$$A_R^{\text{DSD}} = \gamma_R^{\text{DSD}} L \quad (2)$$

where

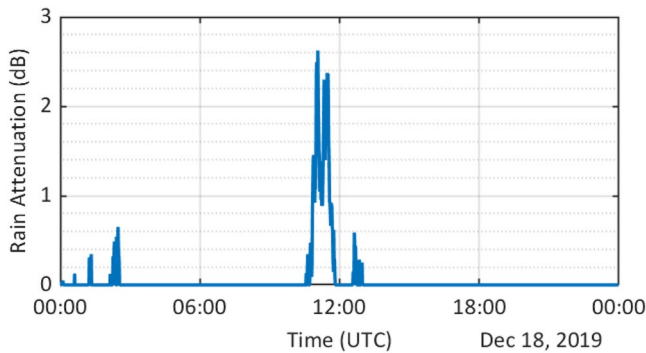
$$\gamma_R^{\text{DSD}} = 4.343 \times 10^3 \frac{\lambda^2}{\pi} \sum_{i=1}^{N_c} \text{Re}[S_0(D_i, f, T, e)] N(D_i) \Delta D_i \quad (3)$$

where  $\lambda$  is the wavelength. Equation 3 basically expresses that the specific attenuation due to rain is obtained by weighting the effect of each drop with diameter  $D_i$ , quantified by the real part of the forward scattering coefficient  $S_0$ , with the associated DSD value  $N(D_i)$ , provided by the disdrometer for  $N_c$  different diameter classes. More specifically,  $S_0$  is calculated using the T-matrix approach proposed in Mishchenko et al. (2002), which is applicable to oblate spheroids. To this aim, the T-matrix method requires as input: the drop diameter  $D_i$ ; the frequency  $f$ ; the water temperature  $T$  (assumed to be 10°C in this work), to calculate the electric permittivity of water; the ratio  $e = a/b$  between the rain drop minor axis  $a$  and major axis  $b$ , derived from (Beard & Chuang, 1987).

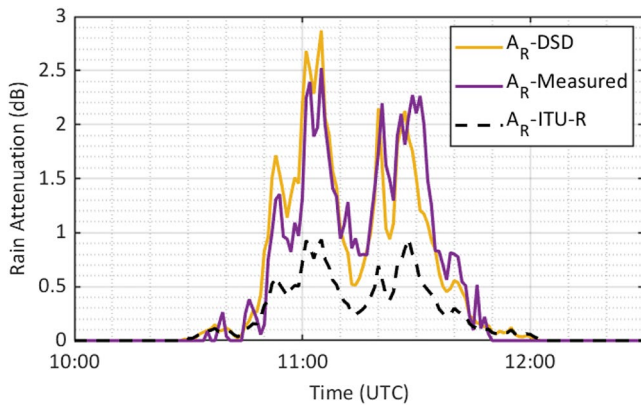
## 4.3. Prediction Results

Figure 9 compares the rain attenuation measured on the link on the 18 December 2019, in Milan, as well as estimated by using the two methods outlined in Sections 4.1 and 4.2. At the beginning of the rain event around 10:30 UTC, both predictions are in good agreement with the link data. However, as the rain rate increases, the discrepancy between the two models clearly emerges: around 11:00 UTC, the DSD offers an accurate prediction (the error is roughly 0.2 dB for the rain attenuation peaks), while the ITU-R P.838-3 based method underestimates the measurements by more than 1.4 dB. This is just an example of how the attenuation due to rain is sensitive to the DSD at D band. Similar results are reported in Figure 10 for a sample rain event occurred in Athens (16 February, 2021): the rain attenuation estimated using the ITU-R P.838-3 based method tends to underestimate the measured data; as mentioned above, the more accurate model reported in Figure 9 is not applicable in this case, as no DSD data are available for Athens.

In order to give a more comprehensive picture of the prediction accuracy, Figure 11 presents the rain attenuation complementary cumulative distribution functions (CCDFs), derived from the link data and estimated using the two methods, for the full two year period in Milan (from 1 February 2018 to 31 January 2020). For the sake of completeness, Figure 12 presents the rain rate CCDF strictly concurrent with the  $A_R$  ones (in other words, rain rate samples are considered in the CCDF only if also the link data are present in the same period). The data availability for the period is 62%, due to some blackouts and some issues with the link equipment: overall, this provides anyway more than one equivalent year of data. The comparison between the curves shows that the DSD approach is more accurate than the ITU-R one for



**Figure 8.**  $A_R$  estimated from local measurements (18 December 2019, in Milan) from the D-band received power.



**Figure 9.**  $A_R$  derived from measurements and estimated using the two prediction methods: 18 December 2019.

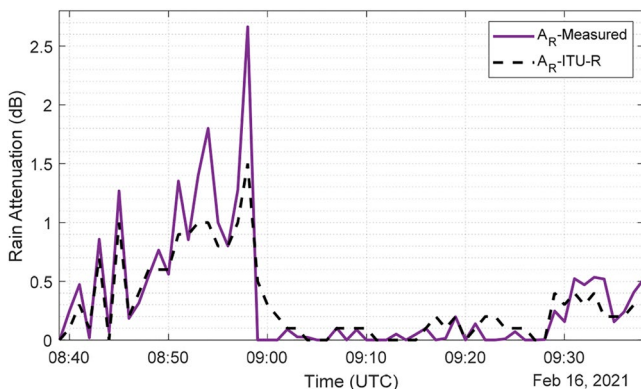


**Figure 10.**  $A_R$  derived from measurements and estimated using the two prediction methods: 16 February 2021, Athens.

exceedance probabilities roughly higher than 0.1%, while the opposite seems to be true for lower probability values. However, it should be highlighted that, as the rain rate gradually increases beyond 10 mm/hr, the rain rate is more and more uneven along the path. This often results in an overestimation of any model assuming that  $R$  is constant (Luini et al., 2018); in fact, in principle, the point measurements of rainfall rate can be above or below the average rainfall rate along the path, but due to the typical exponential shape or rain cells (Luini & Capsoni, 2013), overestimation is typically more likely to occur if  $R$  is assumed to be constant along the path. Given that both approaches are underpinned by this assumption, the overestimation using the DSD approach is expected, while the apparent good agreement between the data and the ITU-R approach actually indicates an underestimation of the latter. This is likely due to the fact that the specific attenuation calculation in Recommendation ITU-R P.838-3 relies on a fixed DSD. The same results are not shown for the data collected in Athens, as in that case, no DSD is available. These data are exploited in the statistical analysis reported in the following Section.

## 5. Rain Attenuation Prediction: Statistical Analysis

The methods presented in the previous section allow estimating the time series of the rain attenuation, but the main drawback of such approaches is obviously the need for the rain rate time series. Indeed, this kind of data is seldom available worldwide, even more so with the necessary temporal resolution (at least 1 min); on the other side, the statistical approach to link design can be achieved with simpler input data and it provides the atmospheric link margin to guarantee a given link availability. This section is devoted to investigating the accuracy of some statistical prediction models, specifically: the model adopted by ITU-R Recommendation P.530-18 (ITU-R P.530-18, 2021), ITU-R Recommendation P.530-18 (2021), typically used as a reference for terrestrial link design and the Lin model (Lin, 1977), already showing a good prediction accuracy when used to estimate rain attenuation statistics at E band (Luini et al., 2020). It is worth remembering that, actually, the application of the ITU-R model is recommended for operational frequencies up to 100 GHz.

Figure 13 presents the two models predictions, when the link electrical and geometrical parameters and the rain rate CCDF shown in Figure 12 are used as input. Also, in all cases, the  $k$  and  $\alpha$  coefficients are calculated by using Recommendation ITU-R P.838-3. Results indicate quite an accurate estimation by the Lin model, while the ITU-R model shows a huge overestimation; this is likely due to the different definition of the path reduction factor in the two models.

In fact, the path reduction factor  $r$  defined in Recommendation ITU-R P.530-18 takes into account the inhomogeneity of the rain rate along the link as a function of rain rate, link length and frequency. Figure 14 provides more details on such a path reduction factor, by showing its value as a function of the path length and rain rate, at 156 GHz: as it turns out, for links shorter than 1 km,  $r$  largely exceeds 1, as better shown on the right side of Figure 14.

On the contrary, as shown in Figure 15, the Lin model defines a path reduction factor that does not exceed 1, even for very short links (tens of meters), and which decreases significantly for high rain rate values (the higher is the rain rate, the more convective is the event, the more uneven is the spatial distribution of the rain rate along the path). This path reduction factor appears to have a more solid physical basis if compared to that in the ITU-R model: in fact, as the path length reduces to some meters, the rain rate is expected to be

constant along the link, that is,  $r = 1$ . In the light of this, we have applied a modified version of the ITU-R model for which the path reduction factor is limited to 1: as expected, the results in Figure 13 (green curve) indicate a much better prediction accuracy in this case.

The same conclusions on the accuracy of the considered models can be drawn from the results obtained using the data collected in Athens (experiment duration from October 2019 to May 2021): Figure 16, reporting the rain attenuation CCDFs on the left side and the input rain rate CCDF on the right side, indicates again an excellent prediction of the Lin model and the modified ITU-R model ( $r$  limited to 1), whereas the original ITU-R model strongly overpredicts the rain attenuation. Considering that Athens and Milan are subject to different meteorological conditions and that the two links have different path lengths, the results shown in this Section corroborate even more the accuracy of the Lin model.

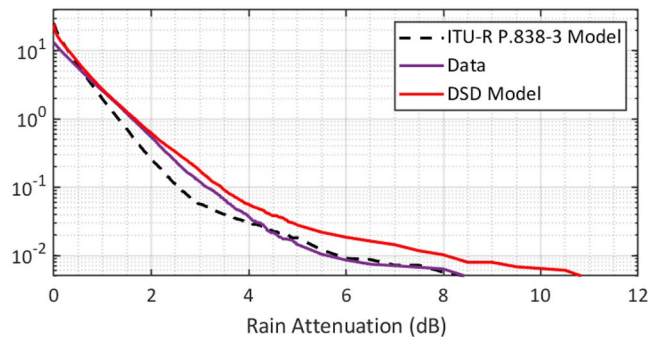


**Figure 11.** Complementary cumulative distribution function of the  $A_R$  from the link data collected in Milan and estimated using the two prediction methods.

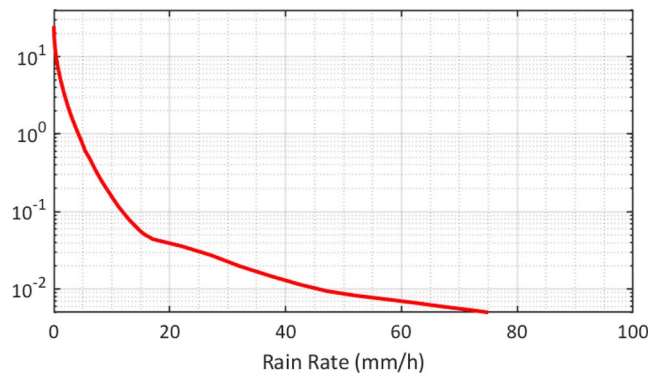


**Figure 12.** Complementary cumulative distribution function of the rain rate from the Drop Size Distribution data in Milan.

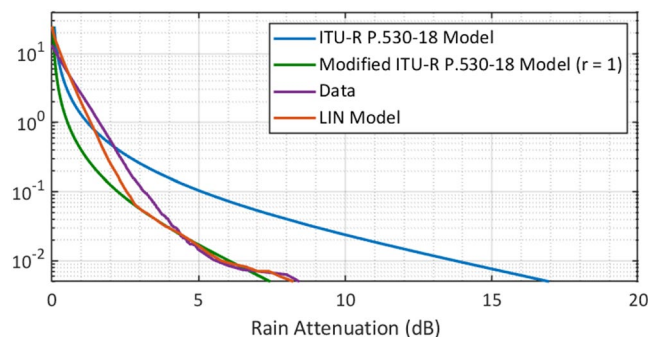


**Figure 13.** Complementary cumulative distribution function of the  $A_R$  from the link data collected in Milan and estimated using the ITU-R P.530-18 and the Lin models.



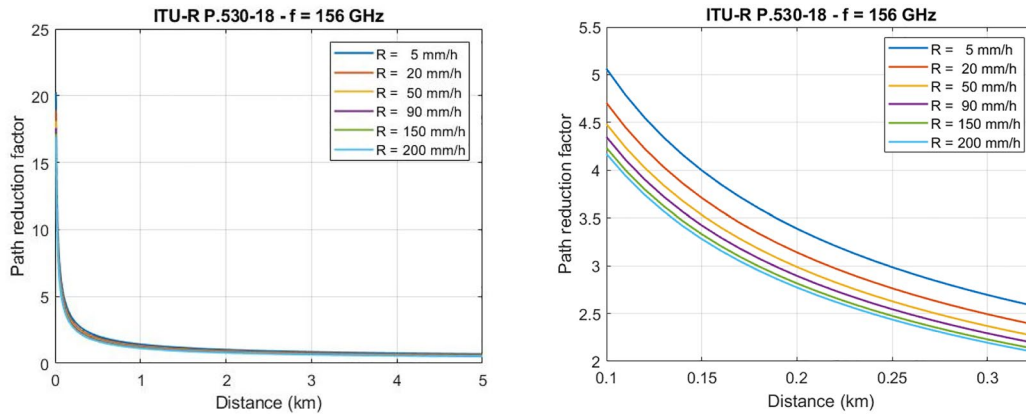


**Figure 14.** Path reduction factor as a function of link length according to the model in Recommendation ITU-R P.530-18.

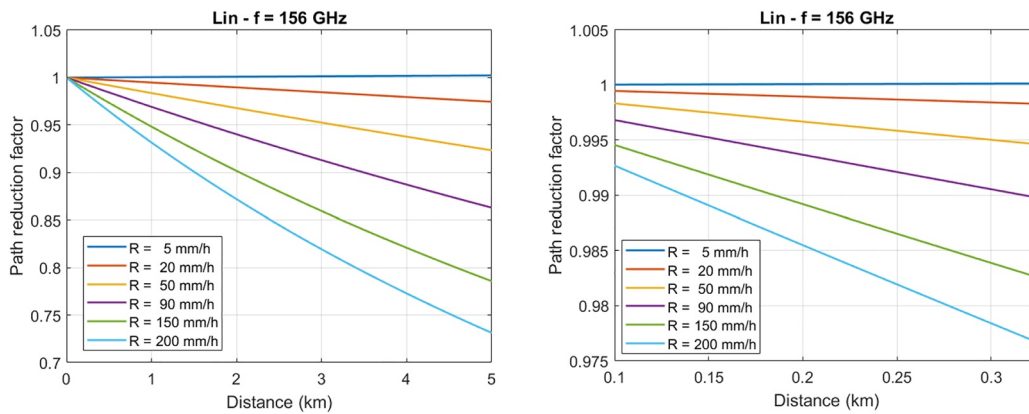


**Figure 15.** Path reduction factor as a function of link length according to the Lin model.

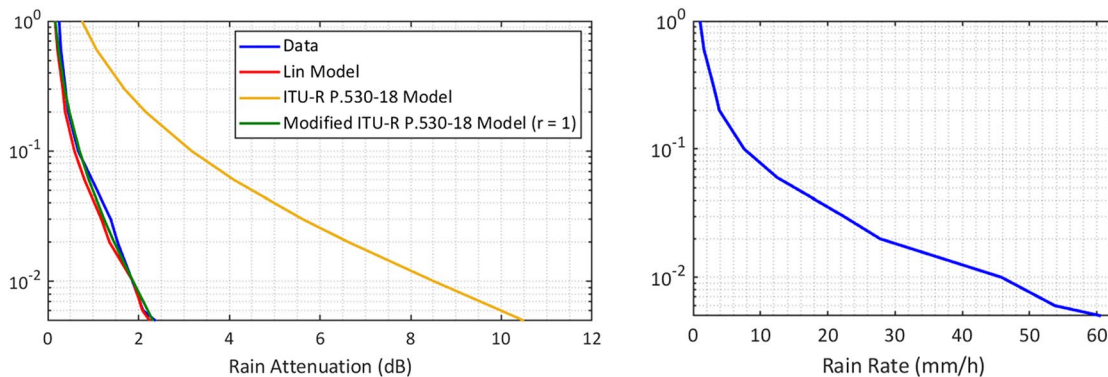


**Figure 16.** Complementary cumulative distribution function (CCDF) of the  $A_R$  derived from the link data collected in Athens and estimated using the model in Recommendation ITU-R P.530-18, and the Lin model (left side) and of the concurrent rain rate CCDF (right side).



**Table 3**  
Accuracy of ITU-R and Lin Rain Attenuation Prediction Models at D Band

	Athens		Milan	
	E (%)	RMS (%)	E (%)	RMS (%)
ITU-R P.530-18 Model	120.3	122.7	34.2	53.5
Lin model	−9.1	10.3	−5.6	11.8

The prediction accuracy of both models can be quantified by using the error figure in ITU-R Recommendation P.311-14 (ITU-R P.311-14, 2013), ITU-R Recommendation P.311-14 (2013):

$$\varepsilon(P) = \begin{cases} 100 \left( \frac{A_m(P)}{10} \right)^{0.2} \ln \left( \frac{A_e(P)}{A_m(P)} \right) & A_m(P) < 10 \text{ dB} \\ 100 \ln \left( \frac{A_e(P)}{A_m(P)} \right) & A_m(P) \geq 10 \text{ dB} \end{cases} \quad (4)$$

where  $A_m$  and  $A_e$  represent the measured and predicted rain attenuation values at the same exceedance probability level  $P$ . Table 3 lists the average (E) and root mean square (RMS) values of the error figure for both models: the results confirm the good accuracy of the Lin model, for which the RMS value is around 10% for both sites. On the contrary, the average value of the error of the ITU-R model is huge (around 50% for Milan and 120% for Athens).

## 6. Conclusions

This work presents the results from a long-term propagation campaign conducted using two short terrestrial links (path length of 325 and 100 m), operating at 156 GHz carrier frequency, installed in Milan, Italy, and Athens, Greece. The impact of precipitation on the two links is investigated by extracting the attenuation due to rain from the received power and by correlating it with the concurrent rainfall data collected at the same sites using disdrometers. Rain attenuation is derived following an accurate approach aimed at isolating rain events, as well as at removing as much as possible the system-induced effects from the attenuation. This is achieved by taking as reference the gaseous attenuation estimated by means of mass absorption models, which requires as input concurrent pressure, temperature and RH.

The analysis of the rain events indicates that the use of the coefficients defined in Recommendation ITU-R P.838-3 to derive specific attenuation from the rain rate tends to underestimate the impact of precipitation, in accordance with the outcomes of Pimienta-del-Valle et al. (2022). On the other hand, the exploitation of the DSD offers a much better prediction accuracy. The statistical analysis has pointed out that, for both sites, the model currently recommended by the ITU-R to predict rain attenuation statistics on terrestrial links (Recommendation P.530-18) yields a significant overestimation for both links, with an average RMS error exceeding 50% and 120% for the data collected in Milan and Athens, respectively. This is due to the unrealistic value of its path reduction factor  $r$ , which largely exceeds 1 for very short links ( $r$  ranging between 15 and 20 for links of tens of meters): indeed,  $r$  should be close to 1 for very short links, that is, when the rain rate can definitely be considered constant along the path. This is reflected by the path reduction factor defined in the model proposed by Lin, which, on the contrary, yields very accurate predictions of rain attenuation statistics in both sites: the RMS error is close to 10% for the data collected in both sites. Considering that Athens and Milan are subject to different meteorological conditions and that the two links have different path lengths, the results derived in this contribution corroborate even more the accuracy of the Lin model, and highlight the need of modifying, for very short links, the prediction model currently adopted in Recommendation ITU-R P.530-18.

## Data Availability Statement

The rain rate and rain attenuation CCDFs data are available in the following public repository: <https://zenodo.org/record/7816983#.ZDVr8vZBybg>. For more information on the data, please contact Lorenzo Luini at [lorenzo.luini@polimi.it](mailto:lorenzo.luini@polimi.it).

## Acknowledgments

None.

## References

- Beard, K., & Chuang, C. (1987). A new model for the equilibrium shape of raindrops. *Journal of the Atmospheric Sciences*, 44(11), 1509–1524. [https://doi.org/10.1175/1520-0469\(1987\)044<1509:anmft>2.0.co;2](https://doi.org/10.1175/1520-0469(1987)044<1509:anmft>2.0.co;2)
- Chen, Z., & Cao, J. C. (2013). Channel characterization at 120 GHz for future indoor communication systems. *Chinese Physics B*, 22(5), 059201. <https://doi.org/10.1088/1674-1056/22/5/059201>
- Ishii, S., Kinugawa, M., Wakiyama, S., Sayama, S., & Kamei, T. (2016). Rain attenuation in the microwave-to-terahertz waveband. *Wireless Engineering and Technology*, 7(02), 59–66. <https://doi.org/10.4236/wet.2016.72006>
- ITU-R Recommendation P.311-14. (2013). Acquisition, presentation, and analysis of data in studies of radiowave propagation.

- ITU-R Recommendation P.530-18. (2021). Propagation data and prediction methods required for the design of terrestrial line-of-sight systems.
- ITU-R Recommendation P.676-12. (2019). Attenuation by atmospheric gases and related effects.
- ITU-R Recommendation P.838-3. (2005). Specific attenuation model for rain for use in prediction methods.
- Kim, S., Khan, W. T., Zajic, A., & Papapolymerou, J. (2015). D-band channel measurements and characterization for indoor applications. *IEEE Transactions on Antennas and Propagation*, 63(7), 3198–3207. <https://doi.org/10.1109/tap.2015.2426831>
- Kim, S., & Zajic, A. (2015). Statistical characterization of 300-GHz propagation on a desktop. *IEEE Transactions on Vehicular Technology*, 64(8), 3330–3338. <https://doi.org/10.1109/tvt.2014.2358191>
- Lam, H. Y., Luini, L., Din, J., Capsoni, C., & Panagopoulos, A. D. (2012). Investigation of rain attenuation in equatorial Kuala Lumpur. *IEEE Antennas and Wireless Propagation Letters*, 11, 1002–1005. <https://doi.org/10.1109/lawp.2012.2214371>
- Lin, S. H. (1977). National long term rain statistics and empirical calculation of 11 GHz Microwave rain attenuation. *Bell System Technical Journal*, 56(9), 1581–1604. <https://doi.org/10.1002/j.1538-7305.1977.tb00582.x>
- Luini, L., & Capsoni, C. (2013). The SC EXCELL model for the prediction of rain attenuation on terrestrial radio links. *Electronics Letters*, 49(4), 307–308. <https://doi.org/10.1049/el.2012.3835>
- Luini, L., Roveda, G., Zaffaroni, M., Costa, M., & Riva, C. (2020). The impact of rain on short E-band radio links for 5G mobile systems: Experimental results and prediction models. *IEEE Transactions on Antennas and Propagation*, 68(4), 3124–3134. <https://doi.org/10.1109/tap.2019.2957116>
- Luini, L., Roveda, G., Zaffaroni, M., Costa, M., & Riva, C. (2018). EM wave propagation experiment at E band and D band for 5G wireless systems: Preliminary results. In *Proceeding of EuCAP*. (pp. 1–5).
- Mishchenko, M. I., Travis, L. D., & Lacis, A. (2002). *Scattering, absorption, and emission of light by small particles*. Cambridge University Press.
- Paraboni, A., Riva, C., Valbonesi, L., & Mauri, M. (2002). Eight years of ITALSAT copolar attenuation statistics at Spino d'Adda. *Space Communications*, 18(1–2), 59–64.
- Pérez-Pena, S., Riera, J. M., Benarroch, A., Pimienta-del-Valle, D., & Garcia-del-Pino, P. (2021). Variability of rain attenuation in the 100-200 GHz band calculated from experimental drop size distributions. In *Proceeding of 15th EuCAP* (Vol. 2021, pp. 1–5).
- Pimienta-del-Valle, D., Riera, J. M., Pérez-Pena, S., Garcia-del-Pino, P., & Benarroch, A. (2022). Characterization of rain attenuation in 80-200 GHz radio links considering non-spherical raindrops. In *Proceeding of 16th EuCAP 2022* (pp. 1–5).
- Saad, W., Bennis, M., & Chen, M. (2020). A vision of 6G wireless systems: Applications, trends, technologies, and open research problems. *IEEE Netw*, 34(3), 134–142. <https://doi.org/10.1109/mnet.001.1900287>
- Thies Klima Laser Precipitation Monitor. (2011). *Document Rev. 2.5. Instructions for Use*.
- Zhang, Z., Xiao, Y., Ma, Z., Xia, M., Ding, Z., Lei, X., et al. (2019). 6G wireless networks: Vision, requirements, architecture, and key technologies. *IEEE Vehicular Technology Magazine*, 14(3), 28–41. <https://doi.org/10.1109/mvt.2019.2921208>